Proceedings World Geothermal Congress 2005
Antalya, Turkey, 24-29 April 2005

Reactive Geothermal Transport Simulations to Study Incomplete Neutralization of Acid Fluid Using Multiple Interacting Continua Method in Onikobe Geothermal Field, Japan

N. Todaka[1], C. Akasaka[1], T. Xu[2], and K. Pruess[2]

1: Geothermal Engineering Group, Electric Power Development Co., Ltd., 6-15-1, Ginza, Chuo-ku, Tokyo, 104-8165 Japan

2: Earth Science Division, Lawrence Berkeley National Laboratory, University of California, Berkeley, CA 94720, USA

norifumi_todaka@jpower.co.jp

ABSTRACT

Two types of fluids are encountered in the Onikobe geothermal reservoir, one is neutral and the other is acidic (pH = 3). It is assumed that acidic fluid is upwelling along a fault zone as incompletely neutralized volcanic fluid. In a previously developed porous medium model (Todaka et al., 2004), the acidic fluid was neutralized due to pH buffering by rock minerals, and acidity was suppressed for a very long time. Here we investigate a multiple interacting continua model (MINC) to examine the role of fracture-matrix interaction for incomplete neutralization in the reservoir. The multi-phase reactive geochemical transport code TOUGHREACT was used. Results indicate very extensive alteration of the primary mineral assemblage in the fracture zone, with significant decrease in porosity and permeability from extensive precipitation of secondary minerals. The secondary minerals may form coatings on the fracture walls, preventing geothermal fluid from further reacting with reactant minerals and maintaining low pH in the fracture zone (incomplete neutralization). It is demonstrated that the MINC model with rock matrix subgridding used in the present study is an important tool for representing fracture-matrix interactions in fractured geothermal systems.

1. INTRODUCTION

The Onikobe geothermal field in northern Honshu, Japan, has been developed by Electric Power Development Co., Ltd. (EPDC). Power plant operation began in 1975 at a capacity of 9 MW, and was increased to 12.5 MW in 1976. The chemical compositions of the production fluids in the Onikobe field vary widely but have certain characteristics in common. The largest variations in concentration are in pH and acid-sensitive constituents including Fe, Mg, Ca that are dissolved from reservoir rocks. There is a strong correlation of low pH with high concentrations of acid-sensitive constituents and Cl (Table 1). The waters separated from reservoir fluids in the ambient condition are grouped into acidic fluid with a pH of around 3 and neutral fluid with a pH between 6.7 and 7.8. Acidic and neutral fluids are locally isolated from one another. The acidic fluid reservoir seems to be limited to deep-intermediate depths close to the central area, based on a spatial relationship between the acidic fluid zone and acidic alteration (kaolinite and pyrophyllite) zone. Neutral fluids with lower salinity are produced from relatively deep horizons penetrated by wells further from the center as well as shallow zone of the center. Acidic fluids in geothermal reservoirs can come from below as incompletely neutralized volcanic fluids. According to Truesdell and Todaka (2004), it is likely that the acidic fluids result from incomplete neutralization of HCl carried in superheated volcanic steam, because the acidic fluid has lower SO_4/Cl ratio and higher chloride than the neutral fluids. In addition, there is clearly a large excess of chloride (defined as chloride greater than that required to electrically balance all the positively charged ions in solution without counting hydrogen) in the acidic fluids. This supports the concept that acid fluids are caused by HCl rising into the geothermal system from a magmatic source at greater depth.

Todaka et al. (2004) indicated that Mn-rich smectite precipitated near the mixing front and that it is likely to form an impermeable barrier between regions with acidic and neutral fluids. Acidic fluid, however, proceeded to neutralize due to pH buffer of rock minerals in the previous porous model and its pH became higher than that of actual field data. In the present paper, a one-dimensional MINC model (multiple interacting continua) with rock matrix subgridding was used to study the incomplete neutralization of acidic fluid in the fractured geothermal reservoir.

Table 1: A range of chemical compositions of acidic and neutral separated waters from the Onikobe production wells. These waters were separated from reservoir fluids in ambient condition.

		Acidic water			Neutral water		
pH		2.8	–	5.0	6.7	–	7.8
H_2S	mg/l	<0.5			<0.5	–	2.1
T-CO_2	mg/l	<10			<10		
Cl^-	mg/l	4300	–	5650	2160	–	4840
SO_4^{2-}	mg/l	19.7	–	50.0	14.7	–	23.9
Na^+	mg/l	1850	–	2240	1100	–	2170
K^+	mg/l	345	–	435	198	–	355
Ca^{2+}	mg/l	474	–	721	179	–	650
Mg^{2+}	mg/l	8.38	–	58.3	0.31	–	5.51
T-Fe	mg/l	1.55	–	371	0.05	–	0.32
SiO_2	mg/l	527	–	725	613	–	695

Sampling: December, 1998

2. SIMULATION APPROACH

2.1 Computer Code

The present simulations were carried out using the non-isothermal reactive geochemical transport code TOUGHREACT, whose physical and chemical process capabilities and solution techniques have been discussed by Xu and Pruess (2001). The simulator can be applied to one-, two-, or three-dimensional porous and fractured media with physical and chemical heterogeneity, and can accommodate any number of chemical species present in liquid, gas and solid phases.

2.2 Kinetic rate law used in the model

For kinetically controlled mineral dissolution and precipitation, a general form of the rate law (Steefel and Lasaga, 1994) is used

$$r_m = \pm k_m A_m \left| \left[\left(\frac{Q_m}{K_m} \right)^{\mu} - 1 \right] \right|^n \quad (1)$$

where m is the mineral index, r_m is the dissolution/precipitation rate (positive values indicate dissolution, and negative values precipitation), A_m is the specific reactive surface area per kg of H_2O, k_m is the rate constant (moles per unit mineral surface area and unit time) which is temperature dependent, K_m is the equilibrium constant for the mineral-water reaction written for the destruction of one mole of mineral m, Q_m is the ion activity product, the exponents μ and *n* are two positive numbers normally determined by experiments, and are usually, but not always, taken equal to unity (as in the present work). The temperature dependence of the reaction rate constant can be expressed reasonably well via the Arrhenius equation (Steefel and Lasaga, 1994) as follows:

$$k = k_{25} \exp\left[\frac{-E_a}{R} \left(\frac{1}{T} - \frac{1}{298.15} \right) \right] \quad (2)$$

where E_a is the activation energy, k_{25} is the rate constant at 25°C, R is the gas constant, and T is the absolute temperature.

2.3 Porosity and permeability change

Temporal changes in porosity and permeability due to mineral dissolution and precipitation can modify fluid flow. This feedback between flow and chemistry is considered in our model. Changes in porosity are calculated from changes in mineral volume fractions. A simple Kozeny-Carman grain model based on spheres was used to calculate changes in permeability due to changes in porosity (Bolton et al., 1999). The Kozeny-Carman equation relates the permeability k (in m^2) to the porosity (ϕ) by

$$k = \frac{R_0^2}{45} \left(\frac{\phi^3}{(1-\phi)^2} \right) \quad (3)$$

where R_0 is the initial local spherical close pack radius. Hence, the ratio of the permeability k to initial permeability k_0 can be expressed as

$$\frac{k}{k_0} = \left(\frac{\phi}{\phi_0} \right)^3 \left(\frac{1-\phi_0}{1-\phi} \right)^2 \quad (4)$$

where ϕ_0 is the initial porosity.

3. PROBLEM SETUP

3.1 Geometric and hydrogeological conditions

We consider an idealized fractured porous medium with two perpendicular sets of planar parallel fractures of equal aperture and spacing. Because of the assumed symmetry only one column of matrix blocks needs to be modeled. A one-dimensional MINC (multiple interacting continua) model was used (Figure 1). Subgrid 1 represents the fracture zone with 1% of the primary grid-block volume. Subgrids 2 through 6 represent the rock matrix with 2%, 10%, 30%, 52.9% and 14.1% volume, respectively. The MINC method can resolve "global" flow and diffusion of chemicals in the fractured rock and its interaction with "local" exchange between fractures and matrix. Details on the MINC method for reactive geochemical transport are described by Xu and Pruess (2001). Our conceptual model should be considered as a small sub-volume of a much more extensive 3-D reservoir. In the vertical direction, the 500 m studied thickness was divided into 20 grid-blocks.

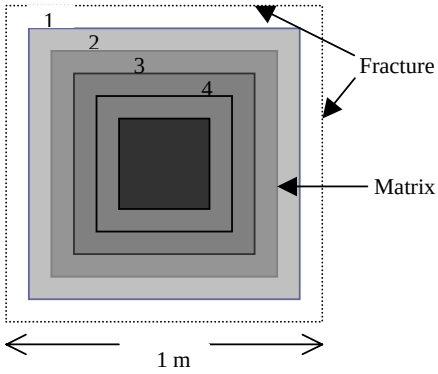

Figure 1. Subgridding of a rock matrix in the method of "multiple interacting continua" (MINC). The figure represents an areal view of a rock matrix column that is surrounded by vertical fractures.

Rock properties in the fracture zone are as follows; grain density: 2740 kg/m^3, porosity: 0.5 (with 50% wall rock), permeability: 1.5×10^{-13} m^2, thermal conductivity: 3 W/(m°C), and heat capacity: 1000 J/(kg°C). Rock properties in the matrix are; porosity: 0.05758, permeability: 1.5×10^{-18} m^2, the other properties are the same as those of the fracture zone. The porosity in fracture and matrix zones was determined by the fact that the total pore volume in fracture and matrix zones is equal to pore volume of the primary grid-block considered in the previous porous medium model.

A constant temperature of 250°C was assumed. The pressure at the bottom boundary was assumed constant 160 bars and 100 bars at top boundary. The amount of water upflowing from the bottom is determined by the applied pressure gradient.

3.2 Geochemical conditions

The acid fluid was applied to the bottom boundary of the model. The neutral fluid was applied as initial conditions in both fracture and matrix zones. Fluid from well 134 was selected as neutral fluid (pH = 5.5 under reservoir conditions), because the water at the separator is neutral (pH = 8.2) at ambient conditions. The acidic fluid was represented by well 130 (Table 2). Chemical concentrations of the two fluids were calculated from separated waters and vapors from the wells using their total specific enthalpies. The agreement between derived enthalpy and geothermometer temperatures suggests that there is little excess steam, consistent with inlet vapor fraction values which are less than 0.1 for almost all samples.

Initial mineral abundances and possible secondary minerals considered in the simulations are listed in Table 3. Possible secondary minerals were determined from field and experimental observations of water-rock interaction and from equilibrium geochemical model calculations. Todaka and Mezaki (1999) employed the batch geochemical code SOLVEQ/CHILLER (Reed, 1982) to analyze the possible secondary minerals in the Onikobe field. Calcite and anhydrite dissolution and precipitation were assumed to take place under chemical equilibrium, whereas those of the other minerals were considered under kinetic conditions. Kinetic parameters k_{25} and E_a (Equation 2) are taken from Ague and Brimhall (1989), Blum and Stillings (1995), Hardin (1998), Johnson et al. (1998), Knauss and Wolery (1989), Nagy (1995), and Tester et al. (1994), or estimated from data therein. The reactive surface areas of minerals are given in the last column of Table 3. The equilibrium constants were taken from the EQ3/6 V7.2b database (Wolery, 1992) which was derived using SUPCRT92 (Johnson et al., 1992). The equilibrium constant of Mn-rich smectite was calculated based on Tardy and Garrels (1974) and Johnson et al. (1992). The chemical composition of Mn-rich smectite is that of the smectite scale formed by fluid mixing in the production well 128 in the Onikobe geothermal field (Ajima et al., 1998).

Table 2: Aqueous chemical concentrations (mol/kg H_2O) of acidic and neutral fluids used for the simulations. Acidic and neutral fluids were sampled from wells 130 and 134, respectively.

component	acidic fluid	neutral fluid
H^+ [a]	3.863×10^{-04}	2.745×10^{-06}
Na^+	6.228×10^{-02}	3.470×10^{-02}
K^+	7.412×10^{-03}	3.814×10^{-03}
Ca^{2+}	1.127×10^{-02}	3.098×10^{-03}
Mg^{2+}	1.143×10^{-03}	5.992×10^{-06}
Al^{3+}	9.577×10^{-06}	5.656×10^{-06}
Fe^{2+}	2.214×10^{-03}	1.491×10^{-06}
Mn^{2+}	5.784×10^{-05}	2.399×10^{-06}
Zn^{2+}	3.376×10^{-05}	1.061×10^{-07}
Pb^{2+}	5.899×10^{-06}	1.000×10^{-12}
Cl^-	9.909×10^{-02}	4.442×10^{-02}
SO_4^{2-}	1.150×10^{-02}	6.500×10^{-03}
HCO_3^-	1.782×10^{-02}	1.372×10^{-02}
SiO_2	8.428×10^{-03}	8.498×10^{-03}
O_2	2.344×10^{-40}	1.724×10^{-40}
temperature (°C)	254	250

[a] activity

Table 3: List of initial mineral volume fractions, possible secondary mineral phases, and their kinetic properties used in the simulation (k_{25}: kinetic rate constant at 25°C, E_a: activation energy and A_m: reactive surface area).

Mineral	Composition	Volume Fraction	k_{25} mol/(m^2s)	E_a kJ/mol	A_m cm^2/g
Primary:					
quartz	SiO_2	0.1477	1.2589×10^{-14}	87.50	98.0
K-feldspar	$KAlSi_3O_8$	0.0495	1.00×10^{-12}	67.83	98.0
albite	$NaAlSi_3O_8$	0.2232	1.00×10^{-12}	67.83	98.0
anorthite	$CaAl_2Si_2O_8$	0.3145	1.00×10^{-12}	67.83	98.0
diopside	$CaMgSi_2O_6$	0.0149	1.00×10^{-13}	67.83	98.0
hedenbergite	$CaFeSi_2O_6$	0.0098	1.00×10^{-13}	67.83	98.0
enstatite	$MgSiO_3$	0.0736	1.00×10^{-13}	67.83	98.0
ferrosilite	$FeSiO_3$	0.0493	1.00×10^{-13}	67.83	98.0
magnetite	Fe_3O_4	0.0176	1.00×10^{-13}	67.83	128.7
Secondary:					
chlorite	$(Mg_{2.5}\,Fe_{2.5})Al_2Si_3O_{10}(OH)_8$	0.0	1.00×10^{-13}	62.76	1516.3
illite	$K_{0.6}Mg_{0.25}Al_{1.8}(Al_{0.5}Si_{3.5}O_{10}(OH)_2$	0.0	1.00×10^{-14}	62.76	1516.3
kaolinite	$Al_2Si_2O_5(OH)_4$	0.0	1.00×10^{-13}	62.76	1516.3
pyrophyllite	$Al_2Si_4O_{10}(OH)_2$	0.0	1.00×10^{-13}	62.76	1516.3
laumontite	$CaAl_2Si_4O_{12}4H_2O$	0.0	1.00×10^{-13}	67.83	98.0
wairakite	$CaAl_2Si_4O_{12}2H_2O$	0.0	1.00×10^{-13}	67.83	98.0
prehnite	$Ca_2Al_2Si_3O_{10}(OH)_2$	0.0	1.00×10^{-13}	67.83	98.0
clinozoisite	$Ca_2Al_3Si_3O_{12}(OH)$	0.0	1.00×10^{-13}	67.83	98.0
epidote	$Ca_2Fe_3Si_3O_{12}(OH)$	0.0	1.00×10^{-13}	67.83	98.0
Mn-rich smectite	$(Ca_{0.17}Na_{0.01}K_{0.01})$ $(Al_{0.18}Mg_{1.74}Mn_{0.85}Fe_{0.03})(Si_{3.87}Al_{0.13})O_{10}(OH)_2$	0.0	1.00×10^{-14}	62.76	1516.3
pyrite	FeS_2	0.0	1.00×10^{-11}	62.76	128.7
sphalerite	ZnS	0.0	1.00×10^{-11}	62.76	128.7
galena	PbS	0.0	1.00×10^{-11}	62.76	128.7
calcite	$CaCO_3$	0.0	at equilibrium		
anhydrite	$CaSO_4$	0.0	at equilibrium		

4. RESULTS AND DISCUSSION

4.1 MINC model

The time evolution of geochemical variables at the central grid-block (225-250 m from the bottom boundary) is selected for the presentation. In the fracture zone, water pH steps down with time (pHs: 5.7, 5.2, 4.1 and 2.9) due to mineral alteration (Figure 2). The pH decreases to 2.9 after chlorite dissolves completely and becomes essentially constant in the entire depth after 100 years (Figure 3). The stable pH of 2.9 is lower than the pH of the bottom upflowing fluid of 3.4. The lower pH is buffered by the steady and slow mineral alteration. All primary minerals except for quartz dissolve and disappear rapidly. Precipitation of quartz and pyrite occurs constantly.

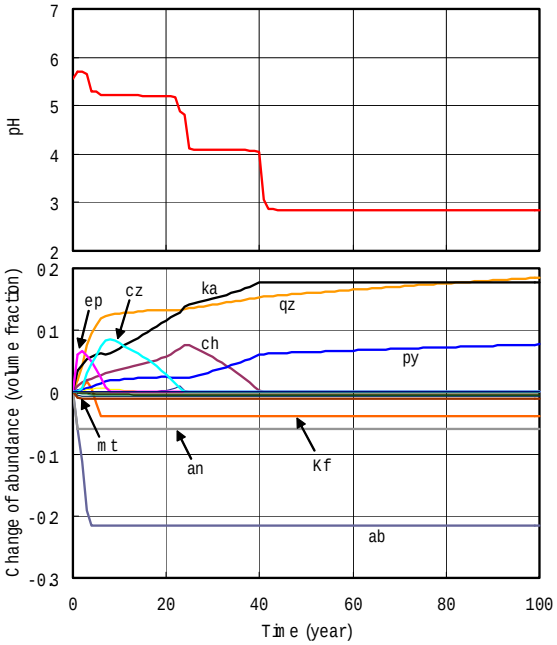

Figure 2: Changes in pH and mineral abundances in fracture zone at the central grid-block (225-250 m), obtained from MINC model. Abbreviations: qz=quartz, ka=kaolinite, py=pyrite, ch=chlorite, ep=epidote, cz=clinozoisite, ab=albite, an=anorthite, Kf=K-feldspar, mt=magnetite.

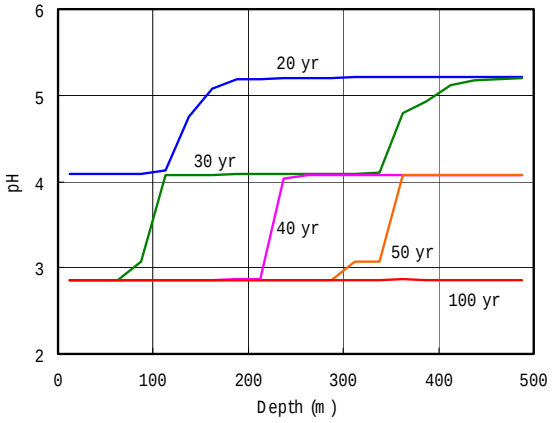

Figure 3: Change in pH of water in fracture zone with time, obtained from MINC model.

In the matrix, the pH remains higher than in the fracture zone (Figure 4). Change in pH from the initial time is not significant. The primary minerals, albite, K-feldspar, chlorite, epidote, and quartz dissolve slowly and are not destroyed after 100 years. Kaolinite and pyrite precipitation occurs also slowly.

In the fracture zone, the porosity decreased from 0.5 at initial time to 0.4 after 100 years at this central grid-block (Figure 5). The permeability decreases from the initial value of 1.5×10^{-13} m^2 to 7.5×10^{-14} m^2 after 100 years. The fact that the permeability change is so modest is due to the very mild dependence of permeability on porosity in Kozeny-Carman relationship.

Decreases in porosity in the fracture zone arise from secondary mineral precipitation. Primary minerals such as pyroxene and plagioclase shortly alter to chlorite, illite and epidote and eventually alter to quartz, pyrite and aluminosilicate minerals such as kaolinite and pyrophyllite. Quartz precipitates directly from geothermal fluid and would be coated on the surface of fracture walls, which might prevent geothermal fluid from reacting with minerals in the matrix. Consequently, the fluid chemistry in the fracture does not evolve much and pH remains acidic. It means that acidic fluid is incompletely neutralized in the fracture zone. Eventually, acidic and neutral fluids would be locally isolated from one another.

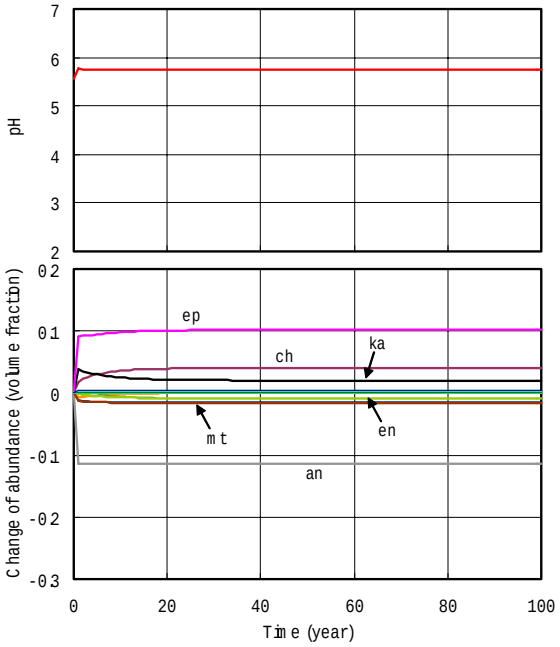

Figure 4: Changes in pH and mineral abundances in the matrix zone contiguous to the fracture zone at the central grid-block (225-250 m), obtained from the porous medium model. 'en' means enstatite. The other abbreviations are as in Figure 2.

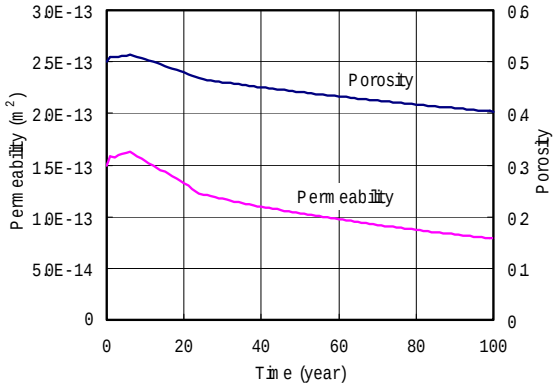

Figure 5: Changes in porosity and permeability in the fracture zone at the central grid-block (225-250 m), obtained from MINC model.

4.2 Comparison with porous model

Results of the previous porous medium model simulation are also presented here for comparison (Figure 6). The porous

model used the same conditions as those of the MINC model. The pH also steps down with time, but much more slowly. The pH becomes essentially constant (2.9) after 39000 years, which is much longer than that of the MINC model (100 years). This is because a large volume of reactant minerals exists for neutralizing in the porous model. The field data indicate that the MINC model would be more realistic than the porous model for the fractured Onikobe reservoir.

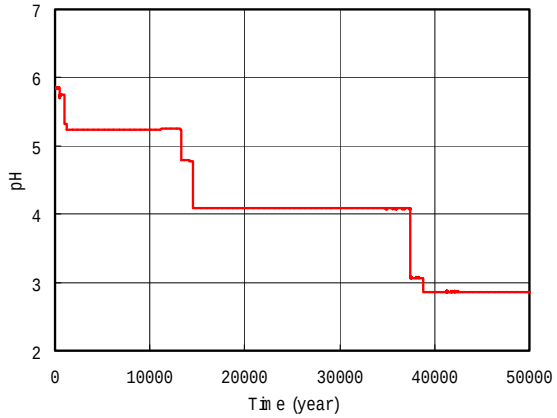

Figure 6: Change in pH at the central grid-block obtained from the porous medium model.

5. CONCLUSIONS

In an earlier porous medium model, acidic fluid proceeded to neutralize due to the large volume of buffer rock minerals. Here we have carried out a one-dimensional MINC simulation, using the reactive geochemical transport code TOUGHREACT, to study the incomplete neutralization of acidic fluid in the Onikobe geothermal reservoir. The MINC model results indicate that porosity and permeability significantly decrease in the fracture zone because of secondary mineral precipitation such as quartz and pyrite. These secondary minerals may coat the surface of the fracture wall, preventing geothermal fluid from further reacting with pH buffer rock minerals and maintaining the low pH value in the fracture zone. In other words, acidic fluid is incompletely neutralized in the Onikobe geothermal reservoir. The MINC model with rock matrix subgridding used in the present study is an important tool for representing the fracture-matrix interactions in the fractured geothermal systems. The reactive transport simulation tool TOUGHREACT and the MINC concept used here may be useful for understanding fluid flow and chemical evolution in other geothermal systems.

ACKNOWLEDGEMENTS

We are grateful to and for a review of the manuscript. We thank John Apps for helpful discussions and suggestions. This work was supported partly by Electric Power Development Co., Ltd. (Japan), and partly by the Assistant Secretary for Energy Efficiency and Renewable Energy, Office of Geothermal Technologies, of the U.S. Department of Energy, under Contract No. DE-AC03-76SF00098.

REFERENCES

Ague, J. J., and Brimhall, G. H.: Geochemical modeling of steady state and chemical reaction during supergene enrichment of porphyry copper deposits, Econ. Geol., 84, 506-528, 1989

Ajima, S., N. Todaka, and H. Murakake, An interpretation of smectite precipitation in production wells caused by the mixing of different geothermal fluids, *Proceedings of Twenty-third Workshop on Geothermal Reservoir Engineering*, Stanford University, Stanford, California, 264-269, 1998.

Blum, A. E., and Stillings, L. L.: Feldspar dissolution kinetics, in Chemical Weathering Rates of Silicate Minerals, chap. 7, edited by A. F. White and S. L. Brantley, Mineral. Soc. Am., 31, 291-351, 1995

Bolton, E. W., Lasaga, A. C., and Rye, D. M.: Long-Term Flow/Chemistry Feedback in a Porous Medium with Heterogenous Permeability: Kinetic Control of Dissolution and Precipitation, *Am. J. Sci., 299*, 1-68, 1999.

Hardin, E. L.: Near-field/altered zone models, Milestone report for the CRWMS M&O, U. S. Department of Energy, SP3100M4: Livermore, California, Lawrence Livermore National Laboratory, 1998.

Johnson, J. W., Knauss, K. G., Glassley, W. E., Deloach, L. D., and Tompson, A. F. B.: Reactive transport modeling of plug-flow reactor experiments: Quartz and tuff dissolution at 240ºC, *J. Hydrol., 209*, 81-111, 1998.

Johnson, J. W., Oelkers, E. H., and Helgeson, H. C.: SUPCRT92: A software package for calculating the standard molal thermodynamic properties of minerals, gases, aqueous species, and reactions from 1 to 5000 bars and 0 to 1000 degrees C, *Comput. Geosci., 18*, 899-947, 1992.

Knauss, K. G., and Wolery, T. J.: Muscovite dissolution kinetics as a function of pH and time at 70°C, Geochim. Cosmochim, Acta, 53, 1493-1501, 1989.

Nagy, K. L.: Dissolution and precipitation kinetics of sheet silicates, Chemical Weathering Rates of Silicate Minerals, 31, 291-351, 1995

Reed, M. H., Calculation of multicomponent chemical equilibria and reaction processes in systems involving minerals, gases and aqueous phase, *Geochim. Cosmochim. Acta, 46*, 513-528, 1982.

Steefel, C. I., and Lasaga, A. C.: A coupled model for transport of multiple chemical species and kinetic precipitation/dissolution reactions with applications to reactive flow in single phase hydrothermal system, *Am. J. Sci., 294*, 529-592, 1994.

Tardy, Y., and Garrels, R. M.: A method of estimating the Gibbs energies of formation of layer silicates, *Geochim. Cosmochim. Acta, 38*, 1101-1116, 1974.

Tester, J. W., Worley, G. W., Robinson, B. A., Grigsby, C. O., and Feerer, J. L.: Correlating quartz dissolution kinetics in pure water from 25º to 625ºC, *Geochim. Cosmochim. Acta, 58*, 2407-2420, 1994.

Todaka, N., Akasaka, C., Xu, T., and Pruess, K.: Reactive Geothermal Transport Simulations to Study the Formation Mechanism of an Impermeable Barrier between Acidic and Neutral Fluid Zones in the Onikobe Geothermal Field, Japan, *J. Geophys. Res.*, 2004 (in press).

Todaka, N., and Mezaki, Y.: Study on silica scale prevention – pH modification technique and geochemical evolution of pH-modified brine in reservoir–, *Chinetsu, 36*, 25-40 (in Japanese with English abstract), 1999.

Truesdell, A. H., and Todaka, N.: Chemistry of neutral and acid production fluids from the Onikobe geothermal field,

Miyagi Prefecture, Honshu, Japan, *Proceedings of an IAEA Coordinated Research Project*, IAEA TECDOC, 2004 (in press).

Wolery, T. J., EQ3/6: Software package for geochemical modeling of aqueous systems: Package overview and installation guide (version 7.0), Lawrence Livermore National Laboratory Report UCRL-MA-110662 PT I, Livermore, California, 1992.

Xu, T., and Pruess, K.: Modeling Multiphase Non-Isothermal Fluid Flow and Reactive Geochemical Transport in Variably Saturated Fractured Rocks: 1. Methodology, *Am. J. Sci., 301*, 16-33, 2001.